Photometric Analysis of the High-Amplitude δ Scuti V2455 Cygni

Elisabeth Banks

A senior thesis submitted to the faculty of
Brigham Young University
in partial fulfillment of the requirements for the degree of

Bachelor of Science

Eric Hintz, Advisor

Department of Physics and Astronomy

Brigham Young University

ABSTRACT

Photometric Analysis of the High-Amplitude
δ Scuti V2455 Cygni

Elisabeth Banks
Department of Physics and Astronomy, BYU
Bachelor of Science

This thesis explores the photomeric analysis of the high-amplitude δ Scuti variable star V2455 Cygni. Long-term observation of this star reveals a strange trend in its O-C diagram which shows evidence of a sudden phase shift in pulsation rather than a continuous change of the period. We observed this star over 126 nights at 2 BYU-affiliated observatories in five filters, and found over 250 times of maximum light for V2455 Cyg in combination with previous publications. We calculated incremental linear regression models to determine when this transition occurred and found that the period was nearly the same before and after this event. This leads us to believe that the change in the O-C diagram was caused by a change in the star's pulsation, either by a change in space motion due to an unseen orbital companion or by a sudden evolutionary "hiccup" in the star's interior which interrupted its usual pulsation. Future analysis of the object's optical and IR spectra should help to support or refute this binary orbital model.

Keywords: variable stars, photometry, δ Scuti

ACKNOWLEDGMENTS

I would like to acknowledge and thank my advisor, Dr. Eric Hintz, for helping to mentor me in research. I would also like to thank the BYU Physics and Asronomy department for the use of telescope time on campus and at West Mountain Observatory.

Contents

Table of Contents v

List of Figures vii

1 Introduction 1
- 1.1 Variable Stars . . . 1
- 1.2 δ Scuti Variable Stars . . . 2
- 1.3 V2455 Cygni . . . 4
- 1.4 Purpose of this Investigation . . . 5

2 Observations and Data Analysis 6
- 2.1 Observations . . . 6
- 2.2 Data Processing and Light Curves . . . 8
- 2.3 Data Analysis . . . 11
- 2.4 Incremental Times of Maximum Light . . . 12

3 Results 14
- 3.1 Observational Baseline for V2455 Cyg . . . 14
- 3.2 Ephemerides and Possible Period Changes . . . 15
- 3.3 Fourier Analysis Results . . . 19
- 3.4 Conclusions and Future Work . . . 20

Appendix A All Times of Maximum Light 22

Appendix B `Period04` Fourier Analysis in Sections 29

Bibliography 35

Index 37

List of Figures

1.1 Sample light curve for δ Scuti type star V2455 Cyg 3

2.1 Field of view for V2455 Cygni 9

2.2 Example light curve for V2455 Cygni 9

3.1 B filter baseline of times of maximum light 15

3.2 V filter baseline of times of maximum light 15

3.3 O-C diagram for linear fit on all *B* filter data 16

3.4 O-C diagram for linear fit on all *V* filter data 17

3.5 O-C diagram for linear fit on V filter 2003-2015 17

3.6 O-C diagram for linear fit on V filter 2015-2021 18

3.7 O-C diagram for linear fit on B filter 2003-2015 19

3.8 O-C diagram for linear fit on B filter 2015-2021 19

Chapter 1

Introduction

1.1 Variable Stars

The basic concept of a variability in stars is that of changing brightness over time. There are several different mechanisms which can cause such changes. Extrinsic variables, such as transiting planets and eclipsing binary systems, occur due to the effects of another object on a star. The type of variables we discuss here are *intrinsic* variables, which means that the changes in brightness are generated by a change in the stars themselves. These types of variables can include novae, supernovae, and pulsating variable stars.

Pulsating variable stars change in brightness periodically over time. They are called pulsating variables because they actually change in size. This change is driven by a layer of ionized gas in the star's interior. When the gas is heated up, it becomes fully ionized and thus more opaque, which traps heat and energy inside the star. In response to this build-up of energy, the outer layers of the star expand outward. As the star expands, it cools down slightly and so changes in temperature and brightness, which produces the periodic variation in light that we observe. This cooling also allows excess electrons in the gas layer to recombine with their atoms, which allows the trapped energy to

escape. Once the pressure has been released, gravity takes over again and collapses the star back down to its original size. This collapse heats and re-ionizes the gas layer inside the star, which starts the cycle over (Carroll & Ostlie 2017).

Some of the most well-known variable stars in astronomy fall under the category of pulsating variable stars. Two specific types, RR Lyrae and Cepheid variables, serve as integral elements of the "distance ladder" which allows us to measure distances across the Milky Way and nearby galaxies. For each type of pulsating variable star, there is a specific mathematical relationship between the star's period of pulsation and its luminosity, or power emitted, which is known as the period-luminosity relation. Using this relationship, we can determine the absolute brightness of a star, independent of distance, by measuring its pulsation period. Because of the inverse-square decay of the intensity of light over distance, we can compare its absolute brightness to what we observe and ascertain the distance to the object. The presence of these stars in star clusters and galaxies outside the Milky Way allows us to more accurately determine how far away they are. Accurate distance measurements play a major role in the way we study and understand the universe.

1.2 δ Scuti Variable Stars

One specific type of pulsating variable star which we observe is the δ Scuti variable star. This category is named after the star δ Scuti, which was one of the earliest of this type to be discovered and distinguished from other short-period variables. A typical light curve for this type of star, and for V2455 Cyg specifically, is shown in Figure 1.1. These stars have spectral type A or F and a period less than 0.3 days, or about 7 hours, with a typical pulsation amplitude of 0.2 magnitudes. Most of this type of star are Population I stars, which means they are more comparable to the Sun in age, with relatively high metallicity. Their pulsations are most likely caused by layers of ionized hydrogen and helium within the stars (Breger 1979). Because their pulsation mechansim is similar

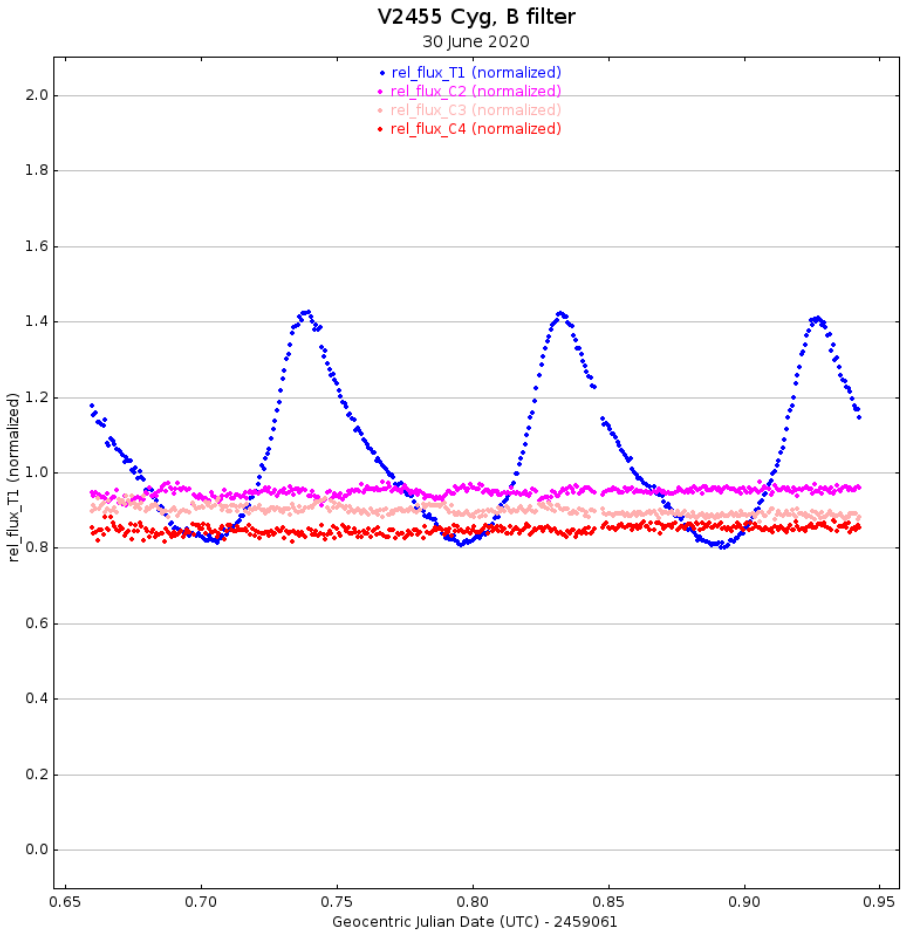

Figure 1.1 Example light curve for the δ Scuti type star V2455 Cyg, in relative flux vs. time. Note the short period, which yields multiple times of maximum light in just one night, and the characteristic curve shape with fast rise and slow decay.

to that of variable stars like Cepheids, δ Scuti stars share the same characteristic pattern of fast rise and slow decay, and they have historically been called dwarf Cepheids.

Like Cepheid and RR Lyrae variables, δ Scuti variable stars have a period-luminosity relationship which makes them valuable targets for determining the distances to star clusters and galaxies (Poro et al. 2021).

The standard method of analysis for δ Scuti variable stars uses the times of maximum light. For each night of data, observers find the time when the star was brightest, which is usually done by

fitting a polynomial fit to the observed light curve and finding the maximum of that fit. A list of all of the times of maximum light is then created and used to develop a model called an ephemeris, which predicts the next time of maximum light. For most δ Scuti stars, the period is constant, and so this model is a simple linear fit. From this model, observers calculate the difference between the predicted time of maximum light and the time when it actually occurred, and construct an O-C (Observed minus Calculated) diagram with the residuals. If there are no clear trends or jumps in the data on this diagram, this means that the linear model was a good fit and the period determined by the ephemeris was correct (Sterken 2005).

1.3 V2455 Cygni

V2455 Cygni, also known as NSV 25610 and BD +46 3325, was first flagged as a potential variable star in a broad stellar kinematic survey in 1991 by Yoss et al. They did not classify its specific variable type or find a period at the time, but simply marked it as a potential variable. Further analysis by Piquard in 2001 classified the star as an SX Phoenicis type variable star with a period of 0.094206 days. Later work by Wils et al. in 2003 for the International Bulletin of Variable Stars (IBVS) revised this classification to δ Scuti based on a new determination of the star's metallicity (relative amount of heavier elements present in the star), and found a very similar period of 0.0942075 d (Wils et al. 2003).

After the star's final classification as a δ Scuti, it was officially named V2455 Cygni in the 78th List of Variable Star Names by Kazarovets et al. 2006. In the following years, more observations of this star were reported by Wils et al. in 2009, 2011, and 2013, and by Joachim Hubscher in the IBVS (Hubscher 2015; Hubscher & Lehmann 2015). Wils et al. 2009 reported new times of maximum light and tested a new method of determining times of maximum light by fitting an average curve to utilize more than just the brightest few data points of each cycle. The other publications by Wils

et al. and the contributions of Hubscher focused on adding additional times of maximum light to create a long baseline of observations for this star.

In 2019, Cruzabeles & Petrov reported on the physical properties of the star as part of a survey on stellar diameters and fluxes, and Peña et al. published three new times of maximum light. Ostadnezhad et al. reported three new times of maximum light in 2020 and combined their measurements with all previous in order to do a long-baseline analysis. They noticed a change in their data compared with previous observations of the star, and their model found a changing period due to an apparent quadratic trend in the O-C diagram.

1.4 Purpose of this Investigation

Researchers here at Brigham Young University (BYU) have been observing V2455 Cygni for several years and have noticed a trend in its O-C diagram corresponding to what Ostadnezhad et al. noticed in 2020. However, as their analysis relied on only three new nights of observation in conjunction with published observations, we believe that their conclusion of a changing period was done incorrectly. BYU has observations of this star from 2009 to 2021, and our data seems to show a different trend in the O-C diagram: a sudden jump rather than a continuous quadratic curve. A quadratic trend suggests a constant change in the period due to ongoing stellar evolution, while a sudden jump suggests a one-time phase shift or interruption instead of a continuous change.

In this investigation, we explore the possibility that the period of pulsation remains the same before and after a certain transition event which introduced a phase shift instead of a constant period change. An abrupt change of this kind could have been induced by a gravitational interaction with an unseen binary companion or a sudden evolutionary event within the star. Gaining a clearer understanding of the cause and nature of this change should help us to better interpret changes in the behavior of variable stars and better understand stellar evolution.

Chapter 2

Observations and Data Analysis

2.1 Observations

The observations taken by BYU astronomers over the last decade were taken at two observatories and included multiple telescopes. Observations were taken at the West Mountain Observatory (WMO) in Payson, UT and Orson Pratt Observatory (OPO) on campus in Provo, UT. The details of the WMO observations (WMO website, "Available Telescopes") and the specifications for the OPO observations are in listed in Table 2.1.

Observatory	Telescope	Diameter (m)	Pixel Scale (arcsec/pixel)
WMO	0.32-m	0.32	0.49
OPO	David Derrick 16-inch	0.4064	0.46 binned 2x2
OPO	10-inch	0.254	0.37 binned 2x2
OPO	8-inch	0.2032	0.57 binned 2x2

Table 2.1 Effective wavelengths for each filter used in this investigation.

Observations were taken over several years at both observatories. Dates observed include nights

in July and August in 2009, 2010, 2011, and 2012, in July through November 2015, in June and October 2016, in December 2017, in July through December 2020, and in August 2021. These observations were taken using the standard Johnson-Cousins filter system, in filters B, V, R, and I in addition to a few observations in the SDSS r filter. By observing V2455 Cyg in multiple wavelengths, we are able to gather more detailed information and compare its behavior in multiple bandpasses of light. The effective wavelength for each Johnson-Cousins filter is listed in Table 2.2 below (Bessell 1990). The effective wavelength for the r filter also listed in Table 2.2 (SDSS website, "SDSS Filters").

Filter	Effective Wavelength (nm)
B	436.3
V	544.8
R	640.7
I	798.2
r	623.1

Table 2.2 Effective wavelengths for each filter used in this investigation.

All observations and times of maximum light which we added to our own were reported by their various observers and published in standard literature for variable stars such as the IBVS. Most of these observations were taken in the Johnson-Cousins B and V filters described above. The majority of our own observations were also in these two filters, which allows us to establish a long baseline of observation for V2455 Cyg.

2.2 Data Processing and Light Curves

The observations taken by WMO and OPO telescopes include three types of standard photometric calibration images in addition to the images of the target object itself. These calibration frames include zeros (or biases), darks, and flats, and each type is meant to correct a different artifact of observation with a digital CCD camera. A standard software package used for this type of image processing is known as the `Image Reduction and Processing Facility` (`IRAF`). The bias level corrects for an artifically-added brightness which is already present on the CCD chip and prevents the analog-to-digital converter from possibly recording a negative value. The dark image is an observation taken with the camera shutter closed, and records the response of the CCD chip to the dark current induced by the camera itself. Because we want to subtract the amount of dark current induced by an exposure of a specific length, the exposure time of the darks should match the exposure time of the images of the target star. The flat image helps to reduce inconsistent pixel responses to light by exposing the entire chip to the same average brightness. We process the images by subtracting the first two types from the object frame and then dividing the result by the flat frame to remove pixel inconsistencies. The result is an image which has been processed by standard `IRAF` procedures using the package `ccdred` (Valdes 1990).

The type of analysis we perform for variable stars such as V2455 Cyg is called photometry: we measure the number of photons that we collect on the CCD chip on each pixel in each image. Each separate frame then becomes a data point of the star's brightness at that time, and putting together several adjacent images in a row allows us to measure the changes in brightness over time. This technique is known as time-series photometry.

To measure the star's brightness on each frame and also account for possible changes and inconsistencies between images, we use a specific type of photometry known as differential photometry, with the software package `AstroImageJ`. On each image frame, we choose several stars whose brightness is stable in time to be comparisons, in addition to the main target star. The comparison

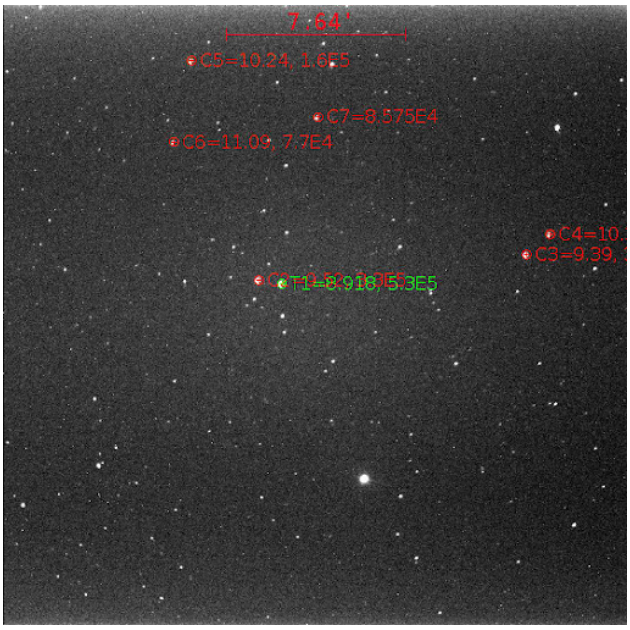

Figure 2.1 Field of view for V2455 Cyg on `AstroImageJ`, ready to begin differential photometry and produce a light curve. The target star is highlighted in green, and the comparison stars are highlighted in red.

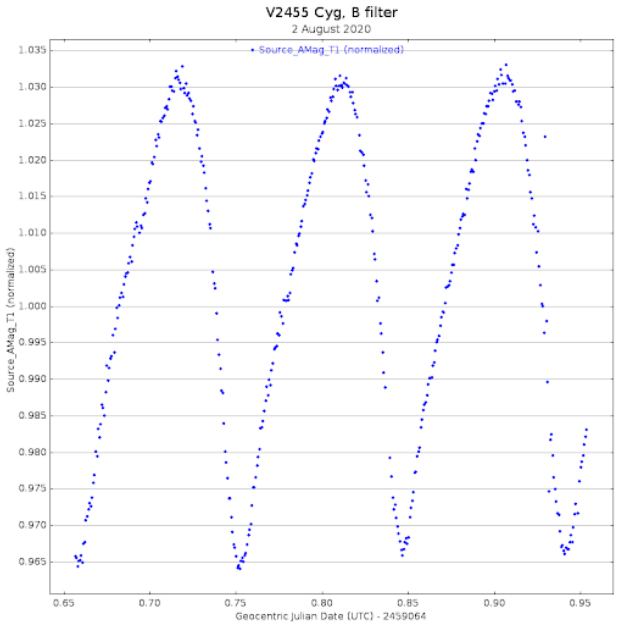

Figure 2.2 Example light curve for V2455 Cyg produced by `AstroImageJ`, taken in August 2020 in Johnson-Cousins B filter. This specific plot shows relative magnitude vs. time and displays three times of maximum light (lower magnitude number is brighter).

stars we used for the analysis of V2455 Cyg are shown in Figure 2.1 and listed with their B and V magnitudes in Table 2.3. The software uses these reference stars to calculate an average brightness for each frame, then measures how much the target star deviates from this brightness. Because we re-calculate this brightness for each frame, we greatly reduce possible errors or inconsistent levels of brightness between subsequent images (Collins et al. 2017). This type of analysis with `AstroImageJ` or a similar program produces a light curve: a graph of brightness vs. time, like the one shown in Figure 2.2.

Identifier	RA	Dec	B mag	V mag
BD +46 3328	21 28 30.01	+46 40 24.99	9.52	9.54
BD +46 3321	21 27 30.23	+46 44 03.60	9.39	9.07
BD +46 3320	21 27 26.06	+46 45 05.11	10.37	9.13
TYC 3590-739-1	21 28 57.44	+46 44 58.33	11.09	9.96
TYC 3590-266-1	21 28 58.03	+46 48 19.54	10.24	9.08

Table 2.3 B and V magnitudes of the comparison stars used in this investigation.

To prepare the data from the light curves for analysis, we need to find and record the times of maximum light, or each time when the star was brightest. Because the pulsation period of V2455 Cyg is so short, there are often multiple times of maximum light on one night, as seen in Figure 2.2. To find the precise time of each maximum, we use a software package called `Peranso` to fit a fifth-order polynomial function to each peak and locate the maximum of the curve. We then record these times of maximum light to be used in fitting a model for the star's pulsation and predicting those in the future.

2.3 Data Analysis

The model we create to predict future times of maximum light is known as an ephemeris. For variable stars with constant periods of pulsation, we use a simple linear model. As discussed in the work of Sterken in 2005, the basic form of this equation is as shown in Equation 2.1:

$$T_{max} = PE + T_0, \tag{2.1}$$

where T_{max} is the next time of maximum light, usually the Heliocentric Julian Date (HJD) , P is the period of pulsation measured in days, E is the cycle number (which number maximum are we on from the very first), and T_0 is the zeropoint, determined by the starting date of the analysis. We begin this analysis by measuring a general starting value of the period so that we can develop a more accurate model. For V2455 Cyg, we used the value from earlier publications, P = 0.094206 days, as the starting period to develop the model. The cycle number, E, of each maximum after the first is calculated based upon this starting value. To test how well the ephemeris fits the observed data, we find a linear regression equation of this form for the data, and then compare the predicted times of maximum to those that actually occurred. At each data point for which we have an observed time of maximum light, we subtract the calculated time in days from the actual time. We plot the residuals on an O-C diagram and look for trends to determine the accuracy of the period and ephemeris (Sterken 2005).

We also perform Fourier analysis of the data collected at OPO from 2009 to 2021 in order to find the fundamental pulsation frequency, f_1, and any overtones. The Fourier analysis was performed using the `Period04` software, which uses a least-squares method to isolate the dominant frequencies. `Period04` uses the fitting formula

$$Z + \sum A_i sin(2\pi(\Omega_i t + \phi_i)), \tag{2.2}$$

to find the major frequencies in periodic observations. We compare these fundamental frequencies and overtones to the ephemeris period generated from the times of maximum light in order to further evaluate the fit of our model. The units of these frequencies are d^{-1}, and so we can find the corresponding period

$$P = 1/f, \tag{2.3}$$

in units of days (Lenz & Breger 2003). If we have performed the O-C analysis correctly and the variable star is not multiperiodic or has a constant period, this value should agree very well with the slope of the ephemeris we found above. In this analysis, we found the major frequencies and overtones for the entire data set as well as for separate sections of each year observed.

2.4 Incremental Times of Maximum Light

One of the major assumptions that motivates our methods of analysis in this investigation is that V2455 Cyg did not have a constantly changing period, but instead displayed an abrupt change in pulsation, then returned to the previous period afterwards. In this situation, we would find a sudden, discontinuous trend in the O-C diagram instead of a smooth quadratic curve. To find the specific transition point, we implemented the linear regression model for the times of maximum light in small, incremental steps.

To do this analysis, we started with the earliest times of maximum light published in the literature by Wils et al., in 2003 and 2009. We found a linear fit for these times of maximum light and created an O-C diagram, which showed that the period had stayed the same between these dates. From here, we added times of maximum light, from our own observations and from the literature, in steps of several months to a year at a time. For each new step, we found a new linear fit for the entire list of maxima up to that point, and then created an O-C diagram for that range. As this process

continued, we began to notice the strange jump trend in the O-C diagram appear only after we added the times of maximum light from 2015. Before that point, the O-C diagram indicated a constant pulsation period, with no visible trends. After that point, the O-C diagram produced by the new linear regression models began to slant downwards and showed evidence of the discontinuous trend.

We then repeated the incremental process with smaller steps within 2015 itself. This closer analysis allowed us to find that the transition point occurred between July and August 2015. To confirm this determination, we did a final linear fit for all of the times of maximum light from 2003 up through July 31 2015. The O-C diagram for this range of dates remained very flat and closely clustered around zero, which indicates that period remained the same throughout all of those years. We then found a linear fit for the times of maximum light from August 2015 on, and found that the O-C diagram for this fit remained flat after the transition as well. Because the period remained the same before and after this point in time, we determined that this was the correct transition point which seems to have introduced a phase shift in the pulsation of V2455 Cyg.

Chapter 3

Results

3.1 Observational Baseline for V2455 Cyg

When we combined our observations here at OPO and WMO with published times of maximum from the literature, we created a long baseline of observation which extends from 2003 to 2021 in the *B* and *V* Johnson filters. A visual timeline of these observations is shown below for each filter, in Figures 3.1 and 3.1 respectively. We also have observations in the other three filters over the course of several years, but the coverage is much more sparse. The long stretch of data allowed us to perform a detailed analysis of the behavior of V2455 Cyg and how its period has changed over time. The full tables of times of maximum light are listed in Appendix A. The *B* and *V* filters constitute the majority of the observations from 2003 to 2021, and so our analysis of the specific event which interrupted the star's pulsation focused on these filters. Observations in all five filters taken at OPO were also used for Fourier analysis to compare the major frequencies found at different wavelengths and evaluate the periods we generated from the ephemeris fits.

Figure 3.1 Timeline of all of the times of maximum light from 2003 to 2021, in the *B* filter.

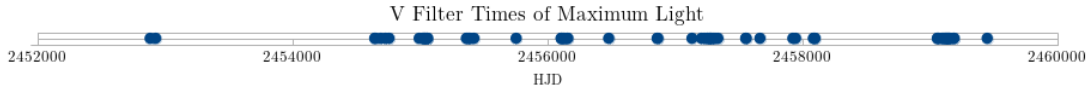

Figure 3.2 Timeline of all of the times of maximum light from 2003 to 2021, in the *V* filter.

3.2 Ephemerides and Possible Period Changes

To produce the O-C diagrams to isolate the jump events, we found initial linear ephemerides for all of the *B* and *V* filter data separately. The linear ephemeris we found for an analysis of all of the *V*-filter times of maximum light is

$$HJD_{max}(E) = 0.09420602E + 2452885.3939, \tag{3.1}$$

and the fit we found for all of the *B*-filter data is

$$HJD_{max}(E) = 0.094206018E + 2452885.3954. \tag{3.2}$$

The O-C diagram generated for each of these fits are displayed in Figure 3.3 and Figure 3.4 (B and V filters respectively), and the jump transition can clearly be observed in the center of each plot (at an HJD of about 2457254 d). The discontinuous jump trend is clearly observed in the center of each plot (at an HJD of about 2457254 d). We located the exact date of this jump by using the incremental O-C method described above in Section 2.4 Before and after this event, the O-C

diagrams appear mostly linear, which would indicate a constant period on each side of the event. To determine whether this model of a "hiccup" in the star's normal pulsation is correct, we used this transition point, the end of July 2015, to generate two separate linear ephemerides to better fit the data.

We started analysis with the V filter data because it had the most consistent coverage and showed a more visible trend. We calculated the first V ephemeris, starting in 2003 and going up through the end of July 2015, as

$$HJD_{max}(E) = 0.09420603E + 2452885.3993, \tag{3.3}$$

for the data up through the end of July 2015 (the transition point) and plotted the O-C diagram for that fit as well, in Figure 3.5. We found that the points on the O-C diagram for the earlier data remained flat up July 31, 2015. This indicates that the period remained the same from 2003 to 2015, with no major changes in pulsation or phase shifts introduced before this event.

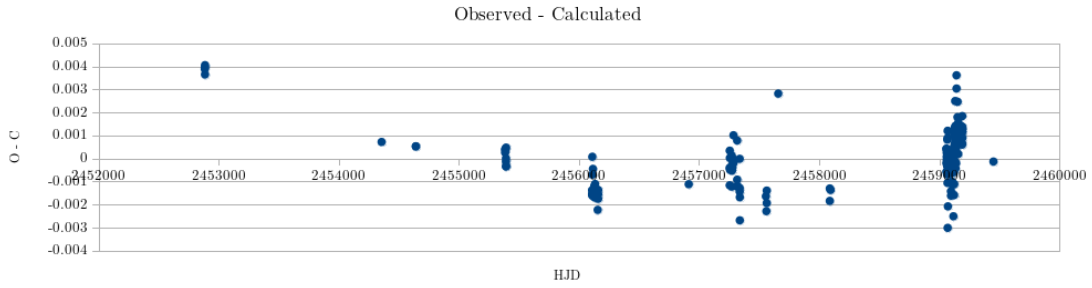

Figure 3.3 O-C diagram for a linear fit of all of the data from 2003 to 2021, in the B filter. Notice the jump trend in the middle; both before and after this event, the graph seems to be linear.

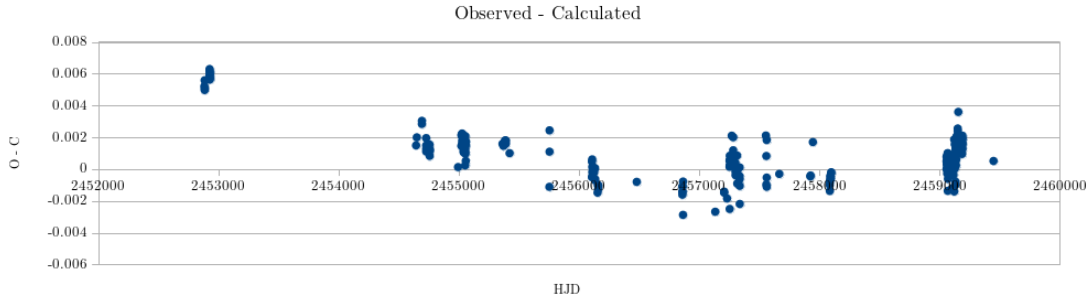

Figure 3.4 O-C diagram for a linear fit of all of the V data from 2003 to 2021, in the V filter. This diagram also displays the sudden jump trend.

With the first section of the V data, which begins in 2003, we fit Equation 3.3, and produced the O-C diagram shown in Figure 3.5. The second ephemeris,

$$HJD_{max}(E) = 0.09420623(E - 46382) + 2452885.3993, \tag{3.4}$$

began in August 2015 and extended to 2021, and produced the O-C diagram shown in Figure 3.6. For the first part of this graph, this analysis supports our initial hypothesis that the period remained the same before and after this event.

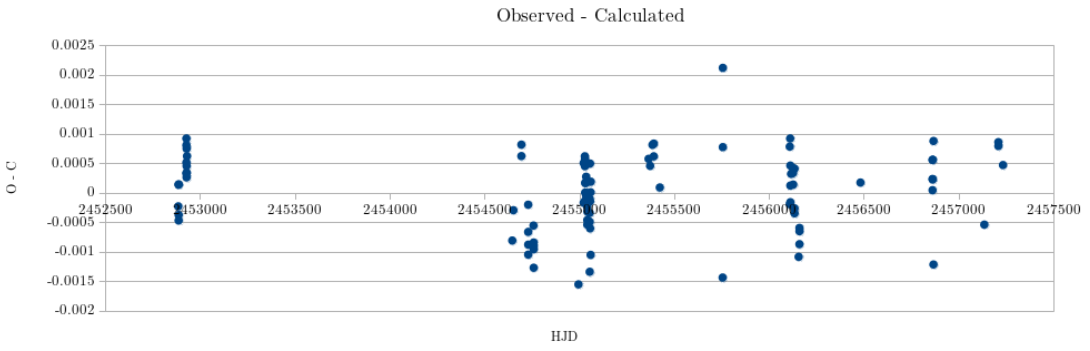

Figure 3.5 O-C diagram for a linear fit of all of the data from 2003 to 2015, in the V filter. The points show a flat trend closely clustered around 0, which indicates a good model fit.

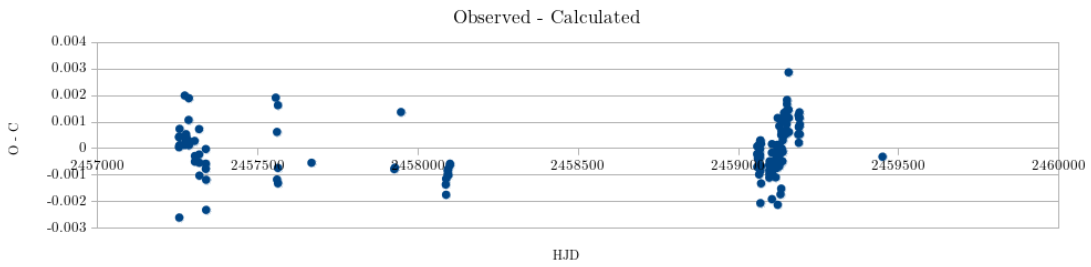

Figure 3.6 O-C diagram for a linear fit of all of the data from August 2015 to 2021, in the *V* filter. The points on the first half of the diagram show a good model fit beginning after the major transition event.

We then repeated this same type of analysis with the *B* filter data. The *B* ephemeris up to July 2015 is

$$HJD_{max}(E) = 0.09420604E + 2452885.3991, \tag{3.5}$$

and the ephemeris after July 2015 is

$$HJD_{max}(E) = 0.09420623(E - 46382) + 2452885.3991. \tag{3.6}$$

Again, we found that the period remained nearly the same before and after this 2015 transition point. The O-C diagrams for the earlier and later sections of the *B* filter data are displayed below in Figures 3.7 and 3.8. In both filters, the interruption of the O-C diagram is due to a sudden event, before and after which the period remains nearly constant.

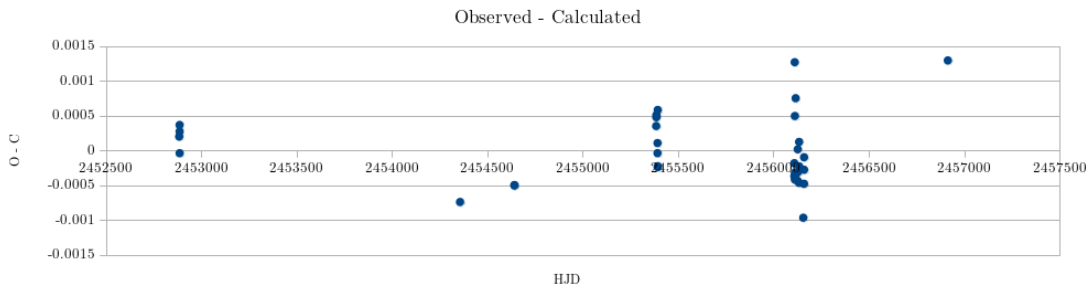

Figure 3.7 O-C diagram for a linear fit of all of the data from 2003 to 2015, in the *B* filter. The flat, near-zero clustering of points indicates a good model fit and a constant period.

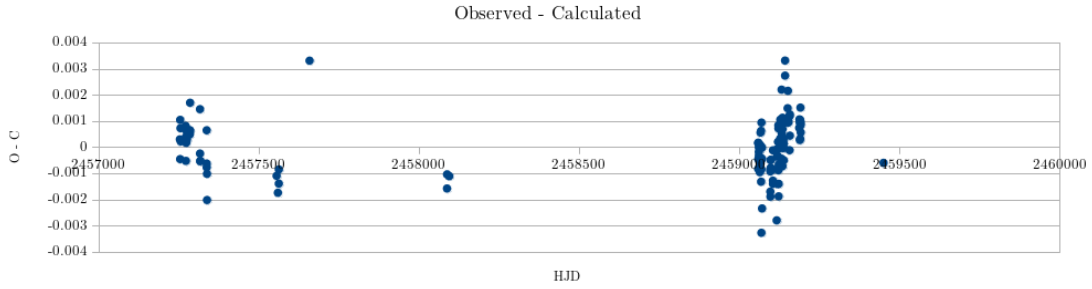

Figure 3.8 O-C diagram for a linear fit of all of the data from August 2015 to 2021, in the *B* filter. The points on the first half of the diagram show a good model fit directly after the major transition event.

3.3 Fourier Analysis Results

In order to confirm the precision and cohesion of the BYU data, we performed Fourier analysis on each year of data, which gave us the major frequencies present in the data. The full list of these frequencies is in Appendix B for reference. Most of the years of data phased together well and had very similar primary frequencies around 10.615 cycles per day, which corresponds to a period of 0.094206 d and matches the periods calculated for this star in literature. The early *V* filter sections, in 2009 and 2010, however, both exhibit strange primary frequencies which are not integer multiples of the more common frequency. After 2010, these frequencies do not show up in any of the *V* data

again; the average fundamental frequency without including these outliers is around 10.614744 c/d, which corresponds to a period of 0.094208581 d. The *B* filter sections, on the other hand, do not display these strange modes in the early data, in 2010 or 2012, where the fundamental frequency and overtones followed the typical pattern. The overall average *B* fundamental frequency was found to be 10.61413 c/d, which corresponds to a period of 0.09421406 d. We are still unsure of what caused these anomalies in the data for the *V* filter, and because it never showed up again, we believe it to be a non-repeating event.

For the *V* filter ephemerides, we found a pre-transition period of 0.09420603 d, which corresponds to a frequency of 10.61503 c/d, and a post-transition period of 0.09420623 d, or a frequency of 10.61501 c/d. For the *B* filter, we found a pre-transition period of 0.09420604 d, with a frequency of 10.61503 c/d, and a post-transition period of 0.09420623 d, with a frequency of 10.61501 c/d. While there is some variation between the major frequencies found in different years of the data and each section has a different number of data points, most of the major frequencies found cluster very closely to these values from the ephemeris model. Our model seems to be a good fit for the data and has found the correct fundamental pulsation frequency.

3.4 Conclusions and Future Work

Our photometric analysis has shown that this transition event appears to be a sudden jump rather than a continuous trend with a changing period. Our current explanations for this change in behavior are either be a sudden change inside the star which interrupted its pulsation only temporarily, or the presence of an unseen binary companion. It is difficult to determine the correct explanation for this phenomenon with photometric analysis alone. Future work on this star by other research group members should include analysis of optical and IR spectra in order to isolate the possible signs of a binary, including spectral features impossible for an F-type star, such as molecular bands, and

periodic changes in the radial velocity indicating an orbit. If no such binary companion is found, we would conclude that this star is undergoing sudden internal changes that affect its outer pulsation, which makes it a very intriguing target. Understanding what disruptions inside a star might cause these “hiccups” in pulsation presents a fascinating new area of research in stellar evolution.

Appendix A

All Times of Maximum Light

Here we display a list of all of the finalized times of maximum light for V2455 Cyg, in the Johnson-Cousins B, V, R, I, and SDSS r filters. This is a combined list including our own observations and published times of maximum light from literature. Attributions for each point are listed below:

Wils 2003	2452885.3991	BYU	2456116.8548084	BYU	2459059.8571381
Wils 2003	2452887.3778	BYU	2456126.8406606	BYU	2459059.9505693
Wils 2003	2452887.472	BYU	2456126.9349496	BYU	2459061.7408147
Wils 2003	2452887.5656	BYU	2456127.876732	BYU	2459061.8351157
Wils 2003	2452887.6599	BYU	2456134.753369	BYU	2459061.9293765
Wils 2003	2452928.2634	BYU	2456134.848248	BYU	2459064.7553625
Wils 2003	2452928.3582	BYU	2456134.941697	BYU	2459064.8493623
Wils 2003	2452928.452	BYU	2456156.702552	BYU	2459064.9438764
Wils 2003	2452928.5465	BYU	2456160.753625	BYU	2459065.6979918
Wils 2003	2452929.2996	BYU	2456160.848107	BYU	2459065.7910674
Wils 2003	2452929.394	BYU	2456160.942257	BYU	2459065.8862894

Table A.1 V filter Times of Maximum Light

Wils 2003	2452929.4885	AAVSO	2456482.468254	BYU	2459066.7337967
Wils 2003	2452929.5823	Hubs Lehm 2015	2456862.401549	BYU	2459066.8275682
Wils 2003	2452931.4667	Hubs Lehm 2015	2456862.49543	BYU	2459066.9221709
Wils 2009	2454357.5561	Hubs Lehm 2015	2456862.589446	BYU	2459068.7124112
Wils 2009	2454642.4354	AAVSO	2456863.437483	BYU	2459068.8064065
Wils 2009	2454642.5296	AAVSO	2456863.532022	BYU	2459068.9011372
Wils 2009	2454646.486	Hubscher 2015	2456867.4869	BYU	2459069.7478626
Wils 2009	2454652.5157	Hubscher 2015	2456867.5832	BYU	2459069.8408559
Wils 2009	2454694.4383	Hubscher 2015	2456914.593	BYU	2459069.9374321
Wils 2009	2454694.5327	AAVSO	2457135.59793	BYU	2459071.7272163
Wils 2009	2454702.4879	AAVSO	2457209.456854	BYU	2459071.8199307
Wils 2009*	2454730.329972	AAVSO	2457209.550995	BYU	2459071.9147828
Wils 2009*	2454730.423717	BYU	2457233.950033	BYU	2459097.6326541
Wils 2009*	2454730.517538	BYU	2457233.950033	BYU	2459097.7271393
Wils 2009*	2454730.611913	BYU	2457254.8658	BYU	2459097.8212067
Wils 2009*	2454758.403015	BYU	2457254.866179	BYU	2459097.9157637
Wils 2009*	2454758.496874	BYU	2457255.80521	BYU	2459098.6695415
Wils 2009*	2454759.344674	BYU	2457255.807922	BYU	2459098.857819
Wils 2009*	2454759.438566	BYU	2457255.902473	BYU	2459098.9519828
Wils 2009*	2454759.5332	BYU	2457255.902473	BYU	2459105.6411247
Wils 2009*	2454995.518589	BYU	2457256.844822	BYU	2459105.7335806
BYU	2455022.8397222	BYU	2457257.880476	BYU	2459105.8298615
BYU	2455022.9346012	BYU	2457257.880476	BYU	2459105.9230101
	2455028.9639	BYU	2457272.766931	BYU	2459117.6992738
BYU	2455029.7173808	BYU	2457272.766931	BYU	2459117.7927961
	2455029.7175	BYU	2457273.895543	BYU	2459120.6195322

Table A.2 *V* filter Times of Maximum Light continued. Points marked * also attr. AAVSO.

BYU	2455030.7530626	BYU	2457273.895543	BYU	2459120.7135413
	2455030.7532	BYU	2457274.837663	BYU	2459121.6562158
BYU	2455030.7533653	BYU	2457274.837663	BYU	2459121.7506017
	2455033.767953	BYU	2457274.932053	BYU	2459122.6927476
BYU	2455033.767953	BYU	2457274.932053	BYU	2459122.78652
BYU	2455035.746073	BYU	2457275.873947	BYU	2459122.8806942
	2455035.7461	BYU	2457275.873947	BYU	2459123.6358243
BYU	2455035.840594	BYU	2457275.873947	BYU	2459123.7267562
	2455040.739032	BYU	2457276.816201	BYU	2459123.8228505
BYU	2455040.739032	BYU	2457276.816201	BYU	2459128.6273345
	2455040.833738	BYU	2457276.910548	BYU	2459128.7226544
BYU	2455040.833738	BYU	2457277.8524909	BYU	2459128.8153414
BYU	2455041.681075	BYU	2457284.823535	BYU	2459132.676741
BYU	2455041.775067	BYU	2457284.918614	BYU	2459132.8667287
BYU	2455041.869044	BYU	2457285.76729	BYU	2459134.6552868
BYU	2455041.963173	BYU	2457285.85972	BYU	2459134.7510176
BYU	2455042.9054532	BYU	2457286.896136	BYU	2459134.8457273
BYU	2455054.77539	BYU	2457303.66486	BYU	2459135.5995253
	2455054.8686	BYU	2457304.606144	BYU	2459135.693059
BYU	2455054.869446	BYU	2457304.6063567	BYU	2459135.788398
BYU	2455054.964041	BYU	2457317.7010774	BYU	2459138.6129771
BYU	2455056.754556	BYU	2457317.702037	BYU	2459138.7081624
BYU	2455056.848119	BYU	2457318.642345	BYU	2459138.8025311
BYU	2455056.941868	BYU	2457318.6428288	BYU	2459139.6500389
	2455059.7676	BYU	2457338.6143177	BYU	2459139.7438097
BYU	2455059.7686611	BYU	2457338.615066	BYU	2459143.6074258

Table A.3 *V* filter Times of Maximum Light continued.

	2455060.7109	BYU	2457338.7087206	BYU	2459143.7019412
Wils 2011	2455365.4676	BYU	2457339.64904	BYU	2459143.7953027
AAVSO	2455365.467788	BYU	2457339.6501753	BYU	2459150.5790645
Wils 2011	2455365.5619		2457556.89283	BYU	2459150.6725452
Wils 2011	2455373.4747	BYU	2457556.892839	BYU	2459150.7666295
AAVSO	2455373.475181	BYU	2457560.8464073	BYU	2459151.6150918
BYU	2455385.9107329		2457560.8482	BYU	2459151.7090398
BYU	2455386.5338854	BYU	2457563.7672363	BYU	2459152.6518641
BYU	2455386.6279817		2457563.7696	BYU	2459152.7462241
BYU	2455392.6933718	BYU	2457563.8608621	BYU	2459153.6878701
BYU	2455392.787794	Pena 2019	2457565.9307	BYU	2459157.6445847
BYU	2455393.5046673	Pena 2019	2457574.8801	BYU	2459157.7401959
BYU	2455393.5978473	Pena 2019	2457575.9157	BYU	2459158.6805396
BYU	2455393.6932732	BYU	2457668.618961	BYU	2459158.7742153
Wils 2011	2455417.5631	BYU	2457926.8379923	BYU	2459187.6954342
BYU	2455424.722893	BYU	2457928.8163767	BYU	2459188.6382215
BYU	2455425.5340429	BYU	2457947.8481293	BYU	2459189.5798403
BYU	2455755.761347	BYU	2458087.6474373	BYU	2459189.6734516
BYU	2455755.761347	BYU	2458088.5891146	BYU	2459190.6164464
BYU	2455756.799825	BYU	2458088.6839222	BYU	2459190.7103211
BYU	2455756.801168	BYU	2458093.5828173	BYU	2459191.5585143
BYU	2456109.7898188	BYU	2458093.6771611	BYU	2459191.6529327
BYU	2456109.8830477	BYU	2458094.6192829	BYU	2459192.5941692
BYU	2456111.8624892	BYU	2458095.6553164	BYU	2459192.6887401
BYU	2456112.7098844	BYU	2458100.5544192	BYU	2459450.9067926
BYU	2456112.8037508	BYU	2458100.6486815		
BYU	2456112.8976751	BYU	2459059.7626477		

Table A.4 *V* filter Times of Maximum Light continued.

BYU	2457317.7010415	BYU	2459122.880182	Wils 2013	2456107.3405
BYU	2457318.6428121	BYU	2459123.6328349	Wils 2013	2456107.4348
BYU	2457338.6142954	BYU	2459123.727519	Wils 2013	2456107.5286
BYU	2457338.7086491	BYU	2459123.8224638	BYU	2455385.91029
BYU	2457339.6503176	BYU	2459128.6279783	BYU	2455386.75827
BYU	2457659.673209	BYU	2459128.7219283	BYU	2455386.85251
BYU	2458088.5892864	BYU	2459128.8171097	BYU	2455392.69274
BYU	2458088.6840323	BYU	2459132.6780721	BYU	2455392.78709
BYU	2458095.6552232	BYU	2459132.7749198	BYU	2455393.72881
BYU	2459059.6678558	BYU	2459132.8674707	BYU	2455393.82302
BYU	2459059.7630426	BYU	2459134.6570462	BYU	2455393.91804
BYU	2459059.856637	BYU	2459134.751037	BYU	2456109.78876
BYU	2459059.9514779	BYU	2459134.8456747	BYU	2456109.88315
BYU	2459061.7410411	BYU	2459135.6000323	BYU	2456111.86293
BYU	2459061.8354217	BYU	2459135.6923839	BYU	2456112.70920
BYU	2459061.9293116	BYU	2459135.7880081	BYU	2456112.80422
BYU	2459064.7553861	BYU	2459138.6134823	BYU	2456112.89751
BYU	2459064.8494589	BYU	2459138.7076847	BYU	2456116.85534
BYU	2459064.9432777	BYU	2459138.8022181	BYU	2456126.83999
BYU	2459065.6979285	BYU	2459139.6499151	BYU	2456126.93431
BYU	2459065.7912549	BYU	2459139.7434748	BYU	2456127.87671
BYU	2459065.8863334	BYU	2459143.6097475	BYU	2456134.75327
BYU	2459066.7342217	BYU	2459143.7033786	BYU	2456134.84771
BYU	2459066.8277904	BYU	2459143.7957902	BYU	2456134.94227
BYU	2459066.9231223	BYU	2459150.5788139	BYU	2456156.70277
BYU	2459068.7120685	BYU	2459150.6729484	BYU	2456160.7541175
BYU	2459068.8073138	BYU	2459151.6149776	BYU	2456160.8485252

Table A.5 *B* filter Times of Maximum Light

BYU	2459068.8995748	BYU	2459151.7096624	BYU	2456160.9429113
BYU	2459069.7479045	BYU	2459152.6523895	BYU	2457254.86603
BYU	2459069.8396844	BYU	2459152.7454215	BYU	2457255.80734
BYU	2459069.9381058	BYU	2459153.6874429	BYU	2457255.90304
BYU	2459071.7266293	BYU	2459157.6443458	BYU	2457256.84479
BYU	2459071.8189464	BYU	2459157.7372528	BYU	2457257.88055
BYU	2459071.9154739	BYU	2459158.6806831	BYU	2457272.76559
BYU	2459097.6320963	BYU	2459158.774078	BYU	2457272.859936
BYU	2459097.7271601	BYU	2459187.695691	BYU	2457273.8006575
BYU	2459097.8212804	BYU	2459188.6380781	BYU	2457273.89579
BYU	2459097.9145227	BYU	2459189.5800179	BYU	2457274.83762
BYU	2459098.6695685	BYU	2459189.6735558	BYU	2457274.93231
BYU	2459098.8576869	BYU	2459190.6163883	BYU	2457276.91028
BYU	2459098.9521991	BYU	2459190.7098732	BYU	2457284.82397
BYU	2459105.6400446	BYU	2459191.5583688	BYU	2457284.91816
BYU	2459105.7341303	BYU	2459191.6531276	BYU	2457285.76586
BYU	2459105.8296179	BYU	2459192.5942386	BYU	2457286.80334
BYU	2459105.9230959	BYU	2459192.6887344	BYU	2457286.89647
BYU	2459117.6027199	BYU	2459450.9065592	BYU	2457317.70274
BYU	2459117.6993576	Wils 2003	2452885.3993	BYU	2457318.64283
BYU	2459117.7938411	Wils 2003	2452887.3777	BYU	2457338.61572
BYU	2459120.6197746	Wils 2003	2452887.472	BYU	2457339.6493161
BYU	2459120.7129154	Wils 2003	2452887.5658	BYU	2457556.88981
BYU	2459121.6565889	Wils 2009	2454357.5561	BYU	2457560.84582
BYU	2459121.7505227	Wils 2009	2454642.4354	BYU	2457563.76657
BYU	2459122.6934886	Wils 2009	2454642.5296	BYU	2457563.86131
BYU	2459122.7875809	Hubscher 2015	2456914.5926		

Table A.6 *B* filter Times of Maximum continued.

BYU	2455385.91112	BYU	2457256.84431	BYU	2457286.89631
BYU	2455386.75835	BYU	2457257.88038	BYU	2457560.84569
BYU	2455386.85237	BYU	2457272.76520	BYU	2457563.7670274
BYU	2455392.69207	BYU	2457273.89522	BYU	2457926.8381123
BYU	2455392.78743	BYU	2457274.83770	BYU	2457928.816162
BYU	2455393.72929	BYU	2457274.93288	BYU	2457947.847717
BYU	2455393.82368	BYU	2457276.91153	BYU	2458088.5892089
BYU	2455393.91789	BYU	2457277.85238	BYU	2458088.6839538
BYU	2457254.86602	BYU	2457284.82316	BYU	2458093.582793
BYU	2457255.80827	BYU	2457284.91764	BYU	2458093.6764944
BYU	2457255.90297	BYU	2457285.76640	BYU	2458095.6558454

Table A.7 *R* filter Times of Maximum Light

BYU	2457233.8560595	BYU	2457273.89503	BYU	2457285.7653274
BYU	2457233.9523098	BYU	2457274.83746	BYU	2457286.89656
BYU	2457254.86606	BYU	2457274.93462	BYU	2457304.6068024
BYU	2457255.80778	BYU	2457276.81567	BYU	2457556.8913308
BYU	2457255.90254	BYU	2457276.91086	BYU	2457557.8313135
BYU	2457256.84496	BYU	2457277.85258	BYU	2457557.9256657
BYU	2457257.88016	BYU	2457284.82441	BYU	2457560.84592
BYU	2457272.7651975	BYU	2457284.91894	BYU	2457563.7671977

Table A.8 *r* filter Times of Maximum Light

BYU	2459139.6496365	BYU	2459151.615393	BYU	2459151.7091896

Table A.9 *r* filter Times of Maximum Light

Appendix B

Period04 Fourier Analysis in Sections

Here we list the Fourier components found for each section of observed data for V2455 Cyg, separated by individual years and done by individual filters. The data in this table was our own observed data from WMO and OPO only.

2009	Frequency (c/d)	Amplitude (mag)	Phase
F1	11.6130182	0.170383346	0.84417
F2	8.61803938	0.0754270948	0.112172
F3	20.2310576	0.0477547914	0.363601
F4	13.1824323	0.036031704	0.431918
2010			
F1	11.0531493	0.172293253	0.599072
F2	20.9461747	0.0646902698	0.598225
F3	10.1784889	0.0525836801	0.239873
F4	9.30268672	0.0378290035	0.0612838

Table B.1 *V* filter major frequencies

2011	Frequency (c/d)	Amplitude (mag)	Phase
F1	10.614701	0.20607612	0.456768
F2	20.2216773	0.05630501645	0.302617
F3	31.8273077	0.0187529941	0.54162
F4	6.07993951	0.012640261	0.418506
2012			
F1	10.6156902	0.20655473	0.969877
F2	21.2294298	0.0583135123	0.533387
F3	31.84512	0.0210833686	0.813861
F4	0.03032367954	0.0194355832	0.27095
2015			
F1	10.6152892	0.18852267	0.0501687
F2	21.2313461	0.546562776	0.282266
F3	31.8470191	0.0211002078	0.0294875
F4	9.62897314	0.0181122716	0.430574
2016			
F1	10.6129402	0.181367708	0.334928
F2	21.2303927	0.052558596	0.840706
F3	4.15132015	0.0261525167	0.859972
F4	6.01038961	0.0227732769	0.970495
2017			
F1	10.614881	0.197258419	0.726687
F2	21.2303369	0.0567630039	0.881584
F3	31.8452179	0.0214025455	0.936008
F4	42.460099	0.00802323178	0.0191478

Table B.2 *V* filter major frequencies continued.

2020	Frequency (c/d)	Amplitude (mag)	Phase
F1	10.6149641	0.198925248	0.614927
F2	21.2299282	0.0564737955	0.650451
F3	31.8445165	0.0197700357	0.664777
F4	1.00595649	0.0195586727	0.626156

Table B.3 *V* filter major frequencies continued.

2010	Frequency (c/d)	Amplitude (mag)	Phase
F1	10.614076	0.247368376	0.91773
F2	21.2281521	0.0712487287	0.254666
F3	31.8467467	0.0252239645	0.677484
F4	42.4563042	0.0107170154	0.7622
2012			
F1	10.6155938	0.258219661	0.78575
F2	21.2302123	0.0709235157	0.546687
F3	31.8448308	0.0268187344	0.212915
F4	0.500349102	0.013101914	0.509131
2015			
F1	10.6151541	0.248195623	0.728119
F2	21.2303081	0.0719264056	0.871379
F3	0.996306884	0.0355953297	0.359984
F4	31.8459343	0.0237075813	0.6269

Table B.4 *B* filter major frequencies

2016	Frequency (c/d)	Amplitude (mag)	Phase
F1	10.6136043	0.226073438	0.389966
F2	21.2272085	0.057939504	0.199205
F3	31.8408128	0.0204206782	0.893204
F4	0.0216696302	0.0174794136	0.680977
2017			
F1	10.6113723	0.253403183	0.569038
F2	21.3707119	0.0751245443	0.690574
F3	31.7002416	0.0246696834	0.568583
F4	9.9631344	0.019250392	0.501467
2020			
F1	10.6149608	0.259749875	0.662279
F2	21.2299216	0.0705850468	0.745069
F3	31.8445067	0.0250982388	0.805737
F4	2.00627569	0.0170055253	0.971012

Table B.5 *B* filter major frequencies continued.

2010	Frequency (c/d)	Amplitude (mag)	Phase
F1	10.6134229	0.157434273	0.758846
F2	21.2313659	0.0467845138	0.0943905
F3	31.8447888	0.0169428115	0.173461
F4	42.4582116	0.00700428578	0.29084
2015			
F1	10.6155667	0.15934156	0.62566
F2	21.2311335	0.0468768702	0.67442
F3	31.8435954	0.0155889277	0.129765
F4	0.0853840554	0.0144956761	0.881559
2016			
F1	10.6168726	0.150021851	0.250712
F2	5.11884929	0.0421565967	0.254803
F3	21.2337451	0.0407751285	0.955575
F4	1.22780159	0.0381170331	0.422448
2017			
F1	10.6150099	0.160016407	0.898609
F2	21.2240999	0.0465233774	0.9331224
F3	0.0929427561	0.0312278384	0.68813
F4	31.8450298	0.0167105681	0.451236

Table B.6 *R* filter major frequencies

2015	Frequency (c/d)	Amplitude (mag)	Phase
F1	10.6149199	0.125387799	0.141843
F2	21.2298398	0.0365443996	0.714992
F3	0.0874933572	0.0157093311	0.765138
F4	31.8447597	0.0119718118	0.180783
2016			
F1	10.6109429	0.120709186	0.910053
F2	21.2263972	0.0351189454	0.0956716
F3	7.04689319	0.0239216326	0.316853
F4	0.257152943	0.0205855817	0.840243

Table B.7 *I* filter major frequencies

2020	Frequency (c/d)	Amplitude (mag)	Phase
F1	10.9479707	0.158385613	0.779728
F2	20.3906983	0.0578954223	0.081508
F3	6.26773382	0.0309681737	0.935324
F4	14.7110786	0.0290173048	0.639811

Table B.8 *r* filter major frequencies

Bibliography

Breger, M. 1979, Publications of the Astronomical Society of the Pacific, 91, 5

Carroll, B. W., & Ostlie, D. A. 2017, An introduction to modern astrophysics, Second Edition

Collins, K. A., Kielkopf, J. F., Stassun, K. G., & Hessman, F. V. 2017, The Astronomical Journal, 153, 77

Cruzabeles, P., & Petrov, R. G. 2019, Monthly Notices of the Royal Astronomical Society, 490, 3158

Hubscher, J. 2015, Information Bulletin on Variable Stars, 6152, 1

Hubscher, J., & Lehmann, P. B. 2015, Information Bulletin on Variable Stars, 6149, 1

Kazarovets, E. V., Samus, N. N., Durlevich, O. V., Kireeva, N. N., & Pastukhova, E. N. 2006, Information Bulletin on Variable Stars, 5721, 1

Lenz, P., & Breger, M. 2003, Communications in Asteroseismology, 146, 53

Ostadnezhad, S., Forozani, G., & Ghanaatian, M. 2020, Research in Astronomy and Astrophysics, 20, 105

Peña, J. H., Rentería, A., Villarreal, C., & Piña, D. S. 2019, Revista Mexicana de Astronomía y Astrofísica, 55, 193

Piquard, S. University of Strasbourg, Strasbourg, France, 2001, Ph.D. dissertation

Poro, A., et al. 2021, Publications of the Astronomical Society of the Pacific, 133, 084201

Sterken, C. 2005, in Astronomical Society of the Pacific Conference Series, Vol. 335, The Light-Time Effect in Astrophysics: Causes and cures of the O-C diagram, ed. C. Sterken, 3

Valdes, F. 1990

Wils, P., van Cauteren, P., & Lampens, P. 2003, Information Bulletin on Variable Stars, 5475

Wils, P., et al. 2009, Information Bulletin on Variable Stars, 5878, 1

—. 2011, Information Bulletin on Variable Stars, 5977, 1

—. 2013, Information Bulletin on Variable Stars, 6049, 1

Yoss, K. M., Bell, D. J., & Detweiler, H. L. 1991, The Astronomical Journal, 102, 975

Index

δ Scuti variables, 2

Ephemeris, 11

Fourier analysis, 11

HJD, 11

Incremental method, 12

Light curve, 10

Observations, 6

Photometry, 8
Pulsation, 1

Times of maximum light, 3, 10

V2455 Cygni, 4
Variable stars, 1